

DUCTILE FRACTURE IN A V/Nb DUAL PHASE STEEL

V. Radmilović, Dj. Drobňjak and M. Rogulić *

The role of martensite in ductile fracture of a V/Nb dual phase steel is studied by means of tensile testing and scanning electron microscopy. The results show that the properties of martensite play an important role in the initiation and propagation of the cracks in a dual phase structure. In addition to the ferrite/inclusions decohesion the crack initiation and propagation by the ferrite/martensite decohesion and martensite cracking control the fracturing process in the presence of a soft low-carbon and a hard high-carbon martensite respectively.

INTRODUCTION

The initiation and propagation of cracks in dual phase steels, in which martensite coexists with ferrite, is not well understood. In addition to microvoid formation at small inclusions (1) and at the ferrite/martensite interface (1-4), the initiation of fracture by cleavage cracks in the ferrite matrix (2,5) and by martensite cracking (2, 3, 6) is also reported. In regard to the propagation mechanism, the void coalescence (1-3), the fracturing of martensite (4, 6) the propagation of ductile crack in the ferrite matrix (2) or martensite (5) is suggested. One or more of these features are associated with the volume fraction of martensite (4, 6), the type of martensite (1), the carbon content (6), the ferrite-martensite size and morphology (2, 5) and the ferrite substructure (7). The purpose of the present paper is to report some results on the effect of the properties of martensite on the crack initiation and propagation in a V/Nb dual phase steel.

EXPERIMENTAL PROCEDURE

Material. The chemical composition of the steel used in this work is given

* Faculty of Technology and Metallurgy, Belgrade, Yugoslavia

(in weight percent) in Table 1. As received material, in the form of a hot

TABLE 1 - Chemical Composition Analysis (Wt Pct)

| C | Mn | Si | P | S | Al | N | V | Nb |
|-------|------|------|-------|-------|-------|-------|-------|-------|
| 0.083 | 1.44 | 0.33 | 0.011 | 0.006 | 0.039 | 0.009 | 0.072 | 0.045 |

rolled bend, is machined into round tensile specimens 4.0 mm in diameter and with 28.0 mm gauge length.

Heat Treatment. Tensile specimens are either step quenched from 800°C (the heat treatment consisted of heating the steel at 800°C for 15 min, quenching into an oil bath at 250°C for 10 min, and water quenching), or directly water quenched from 750°C.

Testing. The heat treated specimens are strained to predetermined strain in an Instron tensile machine at a cross-head rate of 0.1 cm/min. SEM observation are carried out either along the longitudinal cross section of the specimens strained in tension, or on the fractured surface. In a few instances a qualitative microanalysis of selected inclusion is carried out.

RESULTS

The microvoids formation as a function of strain is studied in the step quenched specimens. The results show that a little deformation is required to nucleate microvoids at the ferrite/martensite interface. The first microvoids are observed at $\epsilon = 0.014$ (Fig. 1a). With increasing strain up to the uniform elongation no obvious increase in microvoid population is observed (Fig. 1b, c, d). In a few instances microvoid formation by inclusion decohesion is experienced (Fig. 1a). At and beyond the uniform elongation, in addition to the ferrite/martensite decohesion in the direction of tensile axis (Fig. 2a, b), and ferrite/inclusion decohesion (Fig. 2c), occasional fracturing of martensite is observed (Fig. 2d).

In contrast to the step quenched specimens, an extensive cracking of martensite in the direction perpendicular to the tensile axis, is observed in the directly quenched specimens (Fig. 3a). Also decohesion of the submicroscopic inclusion (Fig. 3c) and decohesion along the ferrite/martensite inter-

face (Fig. 3a, b, c, d) is experienced.

The microanalysis test, which was run on a few microscopic inclusions, showed the presence of one or a few of the following elements: Mn, S, Al.

Observation of the fractured surface revealed two types of dimples in the step quenched structure. The first type in the form of deep cavities is associated with residual microscopic inclusions (Fig. 4a) and/or residual martensite islands (Fig. 4b). The second type of dimples, less than 0.5 μm in diameter, are associated with the submicroscopic inclusions (Fig. 4a). In the directly quenched specimens, in addition to dimples (Fig. 4c), a well defined facets are observed (Fig. 4d).

DISCUSSION

The two heat treatments used in this work, i.e. the step quenching from 800°C and the direct quenching from 750°C, are assumed to produce a dual phase structure with a soft low-carbon and hard high-carbon martensite respectively.

In the presence of the soft low-carbon martensite the ferrite/martensite decohesion, in addition to the ferrite/inclusion decohesion, plays a major role in the initiation and propagation of the cracks. The martensite islands and microscopic inclusions /which are assumed to be either sulfide, oxide or oxi-sulfide/ give rise to the formation of long elongated cavities in the direction of the tensile axis. These cavities as well as microvoids originating from the submicroscopic inclusions /which are assumed to be Nb-carbonitrides/ coalesce giving rise to the formation of the large and small dimples respectively. In short, the martensite islands behave in much the same way as the large inclusions.

In the presence of the hard high-carbon martensite, the martensite cracking, in addition to the ferrite/inclusion decohesion, plays a major role in the initiation and propagation of the cracks. A number of cleavage cracks in martensite give rise to the formation of facets at the fractured surface. However, cracks initiated by fracturing thin martensite plates (denoted by arrow in Fig. 3b) develop into voids by ferrite/martensite decohesion (denoted by arrow in Fig. 3d). These voids coalesce with the voids originating from the inclusions, giving rise to the formation of the dimples, which coexist with the facets at the fractured surface.

SUMMARY

In the presence of a low-carbon martensite, a little deformation is required to nucleate microvoids at the ferrite/martensite interface. The nucleation of voids by decohesion of ferrite/inclusion interface and by cracking the martensite is less frequent. Following the maximum load a number of martensite "inclusions" are completely decohered from the ferrite matrix, contributing in such a way to the crack extension. Crack extension in the direction of the tensile axis which gives rise to the formation of large dimples on the fracture surface, appears to be controlled by decohesion of martensite. In addition to large dimples associated with "inclusions" of martensite and microscopic inclusions, fracture surface is characterized by a number of small dimples, which are associated with submicroscopic inclusions.

In the presence of a high-carbon martensite (obtained by quenching from a temperature low in the $\alpha + \gamma$ range), a well defined facets on the fracture surface, and a number of crack perpendicular to the tensile axis which extends across the martensite, are also observed. This is taken to indicate that cleavage may play an important role in the fracture process, depending upon the properties of martensite.

REFERENCES

1. Marder, A.R., 1982, Met. Trans., 13A, 85
2. Kim, N.J. and Thomas, G., 1981, Met. Trans., 12A, 483
3. Rashid, M.S., 1978, Research Publication GMR-2647
4. Araki, K. et al., 1977, Trans. ISIJ, 17, 701
5. Kunio, T. and Suzuki, H., 1977, Fracture 1977-Proc., vol. 2, 23
6. Davies, R.G., 1978, Met. Trans., 9A, 671
7. Mathy, H. and Gréday, T., 1981, 5th Int. Conf. on Fracture-Proc., vol.2, 739

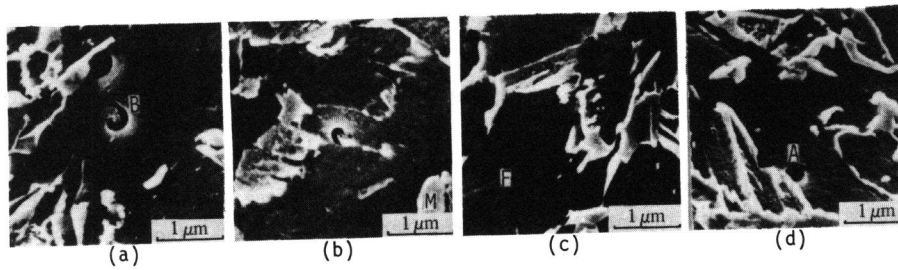


Fig. 1 - Scanning electron micrographs of step quenched samples /strained to: (a) $\epsilon=0.014$; (b) $\epsilon=0.051$; (c) $\epsilon=0.092$; (d) $\epsilon=0.12$ / showing: microvoids at ferrite/martensite interface (denoted by A); microvoids at ferrite/inclusion interface (B); ferrite (F) and martensite (M).

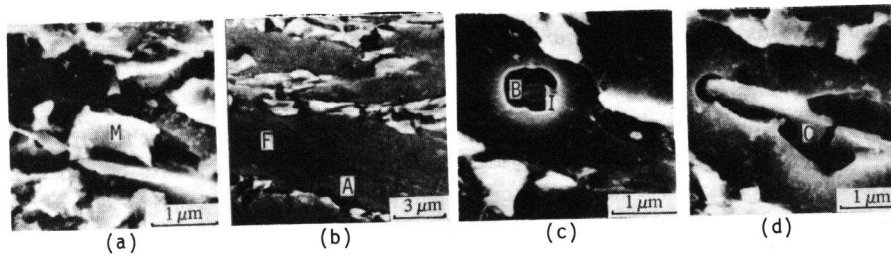


Fig. 2 - Scanning electron micrographs of step quenched samples /strained to: (a) $\epsilon=0.158$; (b) $\epsilon=0.221$; (c) $\epsilon=0.158$; (d) $\epsilon=0.158$ / showing: ferrite/martensite decohesion (denoted by B); ferrite/inclusion decohesion (A); martensite cracking (C); ferrite (F); martensite (M) and inclusions (I).

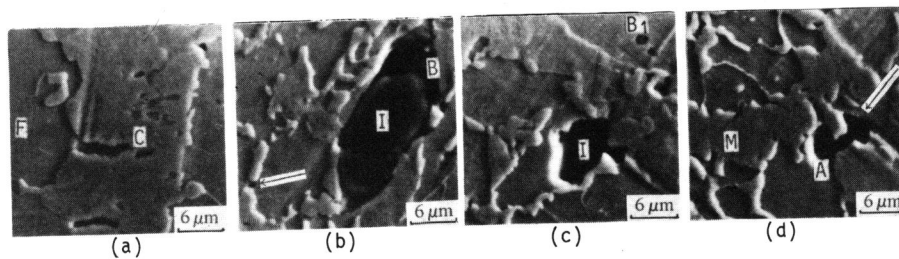


Fig. 3 - Scanning electron micrographs of directly quenched samples /strained to: (a) $\epsilon=0.091$; (b) $\epsilon=0.127$; (c) $\epsilon=0.091$; (d) $\epsilon=0.091$ / showing: ferrite/martensite decohesion (denoted by A); ferrite/microscopic inclusion (B); ferrite/submicroscopic inclusion decohesion (B_1); martensite cracking (C); ferrite (F); martensite (M) and inclusion (I).

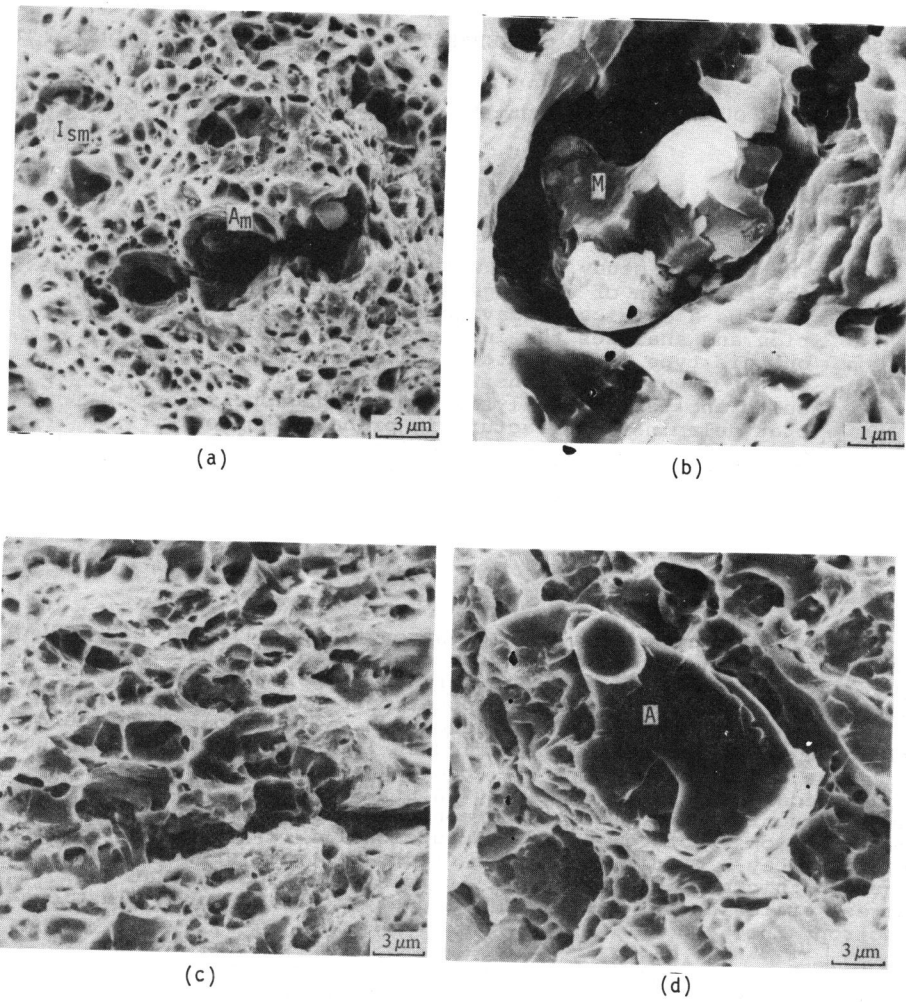


Fig. 4 - Scanning electron fractographs of step quenched (Fig. 1a, b) and directly quenched samples (Fig. 1c, d) showing facets (A) and dimples associated with: residual microscopic inclusions (denoted by A_m); residual martensite (M) and submicroscopic inclusions (I_{sm}).